ACS APPLIED MATERIALS & INTERFACES
Research Article
www.acsami.org

Enhanced Room Temperature Magnetoresistance and Spin Injection from Metallic Cobalt in Co/ZnO and Co/ZnAlO Films

Zhiyong Quan,[†,‡] Xianpeng Zhang,[†] Wei Liu,[†] Xiaoli Li,[†,§] Kiri Addison,[§,#] Gillian A. Gehring,[§] and Xiaohong Xu*,[†]

[†]Key Laboratory of Magnetic Molecules and Magnetic Information Materials of Ministry of Education and School of Chemistry and Materials Science, Shanxi Normal University, Linfen 041004, China

[‡]Department of Materials Science and Engineering, Royal Institute of Technology, Stockholm SE100 44, Sweden

[§]Department of Physics and Astronomy, University of Sheffield, Sheffield S3 7RH, United Kingdom

[#]School of Chemistry, University of East Anglia, Norwich Research Park, Norwich, NR4 7TJ, United Kingdom

ABSTRACT: Co/ZnO and Co/ZnAlO films were prepared by depositing ultrathin cobalt layers and semiconductor layers on glass substrates at room temperature. The films consist of metallic Co particles, semiconductor matrix, and an interfacial magnetic semiconductor with the substitution of Co^{2+} for Zn^{2+} in the ZnO lattice at the interface between Co particles and the semiconductor matrix. Large room temperature negative tunneling magnetoresistance was observed in the films. In addition, the magnetism and magnetoresistance were obviously enhanced by adding aluminum to the ZnO, and in one Co/ZnAlO sample, the room temperature negative magnetoresistance value reaches −12.3% at 18 kOe (compared with −8.4% of the corresponding Co/ZnO film) and the spin polarization of the tunneling electrons is about 37.5% which is characteristic of metallic Co. This enhancement of the tunneling spin polarization has been ascribed to the tunneling through an interfacial magnetic semiconductor, which causes the robust spin injection from cobalt metal into the semiconductors at room temperature resulting from the spin filter effect of the interfacial magnetic semiconductors.

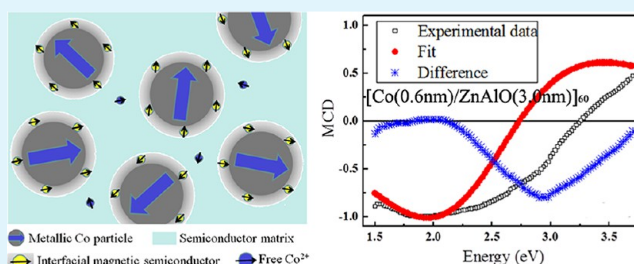

KEYWORDS: *sputtering, interfacial magnetic semiconductors, magnetoresistance, spin polarization, spin filtering*

1. INTRODUCTION

Semiconductor spintronics is expected to be one of the potential technologies which can outperform the conventional semiconductor devices. An important hurdle in the field is the inefficient injection of spin polarized currents from metallic ferromagnets into semiconductors due to the large mismatch in conductivities between them.[1,2] One effective method to overcome this conductivity mismatch obstacle has been done by inserting an insulating tunneling barrier at the interface between ferromagnetic metal and semiconductor layers.[3,4] However, the interface between the insulating layer and the semiconductor layer has quite high recombination rates, which result in a lower spin injection efficiency. Inserting a magnetic semiconductor at the interface between metal and semiconductor layers is regarded as another effective route for spin injection into semiconductors. This effect has been clearly observed in tunnel barriers using EuS but the low Curie temperature (T_c = 16 K) and poor chemical compatibility of these compounds have hindered their use for practical applications.[5−8]

Recently, Gould et al. theoretically demonstrated that the problem of conductivity mismatch can be addressed through the use of dilute magnetic semiconductor contacts.[9] At the same time, the greatest success in this field has been achieved in magnetic semiconductors, in which high efficiency spin injection was demonstrated at room temperature (RT).[10−12] In the case of ZnO-based magnetic semiconductors, the RT ferromagnetism has been obtained through increasing the carrier concentration by doping a few percent of Al.[13−16] Furthermore, the magnetoresistance (MR) effect in inhomogeneous Co−ZnO magnetic semiconductors and in ZnO barrier-based magnetic tunnel junctions have been investigated, which were attributed to spin-dependent variable range hopping[17] and tunneling between (Zn,Co)O electrodes,[18] respectively. Our previous studies have shown that the MR effect, which varies with a different thickness of ZnO layer, originates from spin-dependent tunneling through ZnO barriers in Co/ZnO granular films, and the ZnO electrons themselves may be partially polarized by the metallic Co layer.[19,20] However, it is not clear why the spin-dependent tunneling transport from Co metal into semiconductors can overcome the conductivity mismatch between them. In this work, we investigate in more detail the origin of the MR effect and the high spin polarization of tunneling electrons in Co/ZnO and Co/ZnAlO films with

Received: December 28, 2012
Accepted: April 1, 2013
Published: April 1, 2013

 © 2013 American Chemical Society dx.doi.org/10.1021/am303276b | ACS Appl. Mater. Interfaces 2013, 5, 3607−3613

ZnO (or ZnAlO) thickness of 1.0 and 3.0 nm at RT. The value of RT MR in the Co/ZnAlO film with ZnAlO thickness of 1.0 nm reaches −12.3% (compared with the value of −8.4% in the Co/ZnO film with ZnO thickness of 1.0 nm), and the corresponding spin polarization is about 37.5% equaling that of metallic Co. The enhanced spin injection from a metal into a semiconductor may be due to the formation of the magnetic semiconductors at the interface between the metallic Co particles and the semiconductor matrix in the granular films, which can act as a spin filter. The larger spin injection from metallic Co particles into ZnAlO matrix indicates the larger spin filtering of the interfacial magnetic semiconductors by Al doping. In addition, we found a small MR in a Co/ZnO/Ag junction with one magnetic electrode at RT suggesting the interface between metallic Co and ZnO layer is a magnetic spin filter barrier.

2. EXPERIMENTAL DETAILS

Co/ZnO and Co/ZnAlO films were made by sequentially depositing ultrathin Co layers and semiconductor layers on glass substrates for 60 periods at RT by magnetron sputtering. The nominal structures are $[\text{Co (0.6 nm)/ZnO } (x \text{ nm})]_{60}$ (denoted as Co/ZnO) and $[\text{Co (0.6 nm)/ZnAlO } (x \text{ nm})]_{60}$ (denoted as Co/ZAO), where $x = 1.0, 3.0$. The ZnAlO layer was prepared with a composite target of a ZnO ceramic containing four small Al pieces on the surface. The Al concentration for the ZnAlO film was estimated to be about 2 at. % using the energy dispersive spectroscopy (EDS). Details of the growth have been described in a previous publication.[20] The structure was determined by X-ray diffraction (XRD) and transmission electron microscopy (TEM). The magnetic field dependence of MR was measured using a conventional four-probe method with current in the plane at RT. The magnetic properties of the films were measured using a superconducting quantum interference device magnetometer (SQUID) with a magnetic field applied parallel to the film plane. The magneto-optical spectra were taken with a Xe lamp and monochromator with a photoelastic modulator. The chemical state of Co in the films was investigated by X-ray photoelectron spectroscopy (XPS) using Al Ka X-ray source.

3. RESULTS AND DISCUSSION

From the XRD patterns of the Co/ZnO and Co/ZAO films (not shown), there is no signal of a peak from metallic Co in any of the films suggesting that the Co particles in four films are too small to be detected by means of XRD. A broad ZnO (002) peak is just discernible in the Co/ZnO (3.0 nm) film as well as the Co/ZAO (3.0 nm) film. Figure 1 shows the TEM plane view bright-field micrograph for Co/ZnO and Co/ZAO films with $x = 1.0$. It can be seen that the films have a similar structure consisting of Co nanoparticles (dark regions) dispersed in a semiconductor matrix (light regions). Most nanoparticle sizes range from 3 to 6 nm in diameter in the granular films. In our experiments, Co does not wet the semiconductors and consequently breaks up into nanoparticles, which is due to the fact that the surface energy of metallic Co (∼2.52 J/m^2) is higher than ZnO (∼1.58 J/m^2). Remarkably, the interface between Co particles and semiconductor matrix is not distinct, probably implying a transition region between them, which will be discussed below.

We now turn toward the MR effect of the films. The observed RT MR for the granular films in the maximum applied magnetic field of 18 kOe is shown in Figure 2. Here, the MR ratio is defined as follows:

$$\text{MR}(H) = [R(H) - R(0)]/R(0)$$

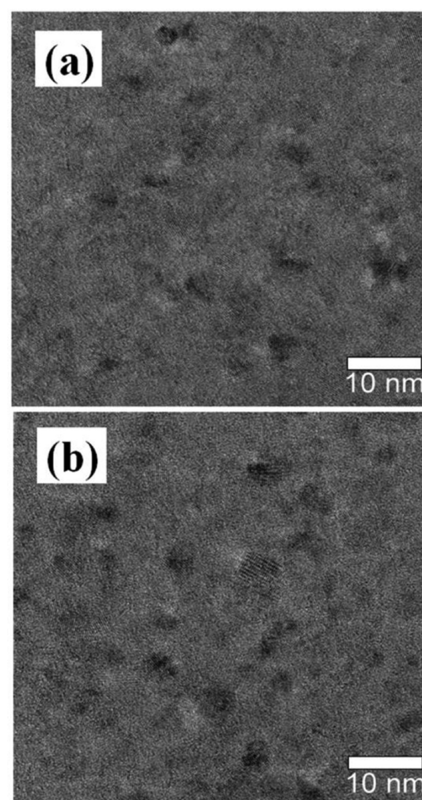

Figure 1. TEM plane view images for the Co/ZnO (1.0 nm) film (a) and Co/ZAO (1.0 nm) film (b).

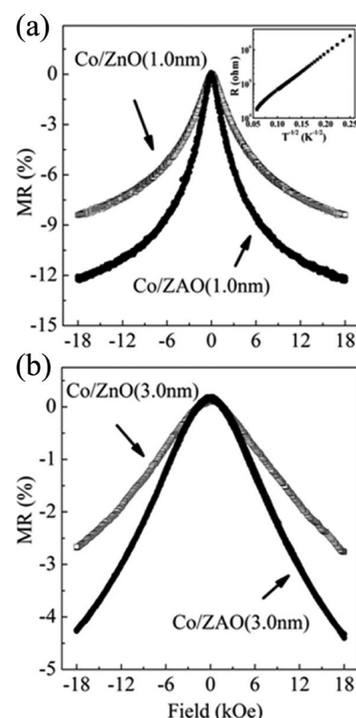

Figure 2. MR measured at RT as a function of field for the four granular films measured up to 18 kOe with $x = 1.0$ (a) and 3.0 (b). The inset of (a) shows the temperature dependence of the resistance (R) of the Co/ZAO (1.0 nm) film.

where $R(H)$ and $R(0)$ are the resistances in an external magnetic field and zero field, respectively. It can be seen that

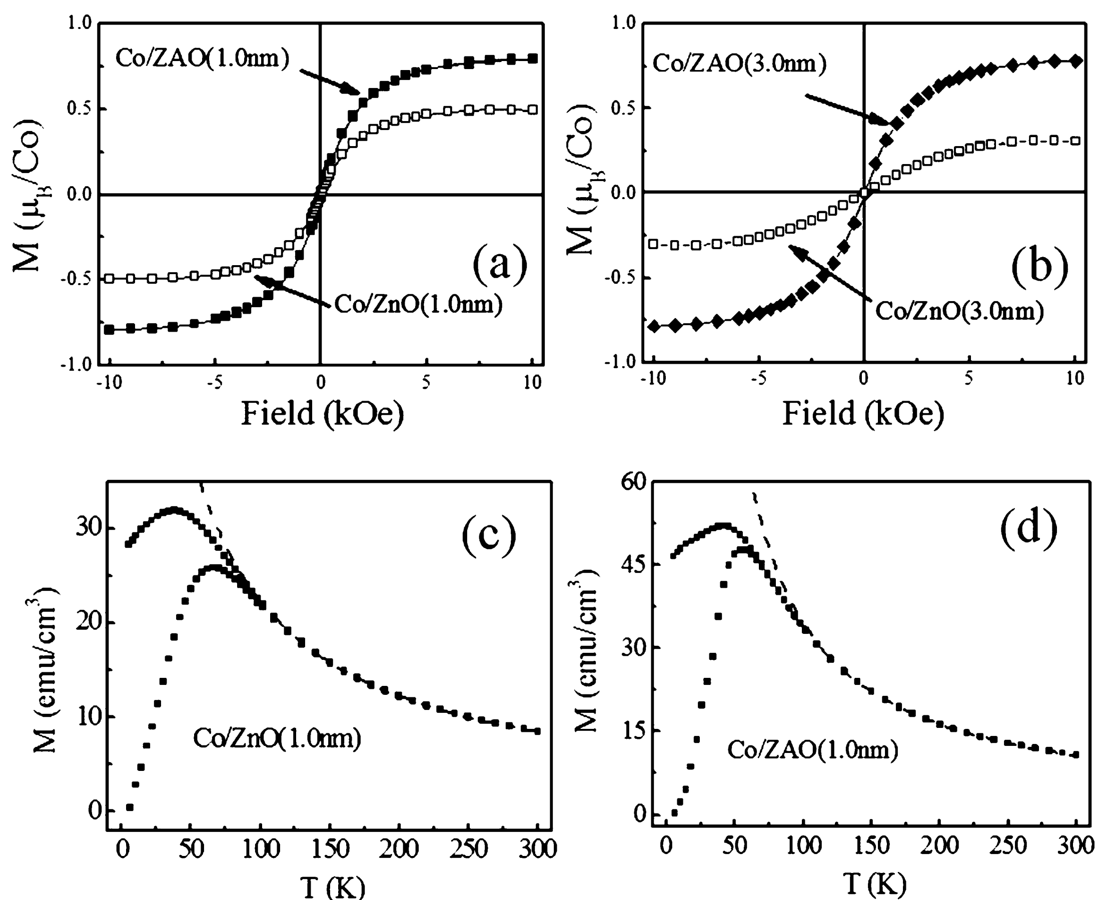

Figure 3. RT magnetization of the Co/ZnO and Co/ZAO films with x = 1.0 (a) and x = 3.0 (b). Temperature dependence of the ZFC−FC magnetization for the Co/ZnO (c) and Co/ZAO (d) films with x = 1.0 in 100 Oe field with the diamagnetic signal from the glass substrates subtracted; the dashed curves are the Curie−Weiss fitting to the high temperature regions of the plots.

the RT MR values of Co/ZnO films are −8.4% and −2.7% for x = 1.0 and 3.0, respectively. For the Co/ZAO films, the value is considerably larger than that of the corresponding Co/ZnO films. The MR of Co/ZAO film with x = 1.0 reaches −12.3% at RT. As shown in the inset of Figure 2a, the temperature dependence of the resistance (R) of the Co/ZAO (1.0 nm) film almost follows ln $R \propto (T_0/T)^{1/2}$. This result suggests that the electron transport in the sample is via interparticle tunneling.[21]

A rough estimate of the spin polarization in these films can be obtained from the Inoue−Maekawa model as follows:[22]

$$\mathrm{MR} = P^2m^2/(1 + P^2m^2)$$

where P is the spin polarization of the tunneling electrons, m is the relative magnetization of the film, and m^2 = $\langle\cos\theta\rangle$. In the saturated state, m = 1, and then, the above equation becomes MR = $P^2/(1 + P^2)$. The RT spin polarization calculated from the MR value of −8.4% for the Co/ZnO (1.0 nm) film is about 30.2%, and it increases up to about 37.5% for the MR of −12.3% obtained in the Co/ZAO (1.0 nm) film. The spin polarization of electrons at the Fermi level of bulk Co metal was reported to be 35% determined by tunneling and 37% measured by Andreev reflection in Co−Pb thin film nanocontact.[23] This indicates that the transfer of polarized carriers from Co metal particles into the semiconductors is extremely efficient in the Co/ZAO film. Besides, we believe that the spin polarization value of cobalt only sets lower limits and its actual value may be higher. This is because the MR curve is not completely saturated at 1.8 T as shown in Figure 2, and the MR ratio might obtain a higher value if a higher magnetic field were applied to our samples.

Figure 3a,b shows the RT magnetization of Co/ZnO and Co/ZAO films after subtracting the linear diamagnetic and paramagnetic background. It can be seen that the saturation magnetization for the Co/ZnO films are 0.49 μ_B/Co and 0.31 μ_B/Co for x = 1.0 and 3.0, respectively. In the case of the films with Al doping, the saturation magnetizations are enhanced to 0.79 μ_B/Co and 0.78 μ_B/Co for x = 1.0 and 3.0, respectively. It should be pointed out that the enhanced magnetism of the Co/ZAO films corresponds to larger MR and enhanced spin polarization compared with the Co/ZnO films, as shown in Figure 2. The zero-field-cooled and field-cooled (ZFC−FC) magnetizations of the Co/ZnO and Co/ZAO films with x = 1.0 are shown in Figure 3c,d. The diamagnetic signal from the glass substrates was subtracted from the data. At high temperatures, the curves can be fitted by a Curie−Weiss law, $\chi = C/(T-\theta)$, where C and θ are the Curie constant and the Curie−Weiss temperature, respectively. The FC plots start to deviate from the Curie−Weiss law at temperatures above the blocking temperature (T_b) identified by the maximum in the ZFC plots, revealing that a mixed magnetic phase may exist.[24] The above Curie−Weiss fit gives a negative Curie−Weiss temperature value of −21.2 K for the Co/ZnO (1.0 nm) film suggesting the presence of an antiferromagnetic interaction and a positive value of 10.5 K for the Co/ZAO (1.0 nm) film indicating ferromagnetic interaction. An approximate value for the average moment of nanoparticles, m_c, may be obtained by combining

the saturation magnetization, $M_{sat} = Nm_c$, and the Curie constant $C \propto Nm_c^2$, where N is the number of magnetic particles per unit volume. The average moment values obtained in this way are 1.01×10^{-16} and 0.66×10^{-16} emu for the Co/ZnO (1.0 nm) and Co/ZAO (1.0 nm) films, respectively. Another estimate may be obtained by estimating the mean volume of magnetic particles from T_b; assuming that both the anisotropy (K) and the magnetization per unit volume of the nanoparticles were those of bulk Co metal, we use $KV = 25k_BT_b$, where $K = 2.7 \times 10^{-5}$ J/m^3 is the magnetic anisotropy constant, V is the average volume of the nanoparticles, and k_B is Boltzmann constant. This procedure gives the average moment value of nanoparticles of 1.13×10^{-16} and 0.96×10^{-16} emu for the Co/ZnO (1.0 nm) and Co/ZAO (1.0 nm) films, respectively. The deviation of the moment values between these two estimates for the Co/ZnO and Co/ZAO films indicates that the magnetism of the films may not come just from metallic Co particles and it should be related to a mixed magnetic phase. This is consistent with the result of ZnO/CoFe multilayers reported by Huang et al.,[24] who demonstrated a mixed structure consisting of two parts: diluted magnetic semiconductors and superparamagnetic CoFe clusters.

The magnetic circular dichroism (MCD) was used to further investigate the origin of the magnetism and robust spin injection in the films. Figure 4 shows the MCD spectra for the Co/ZnO and Co/ZAO films with $x = 3.0$ measured at RT. For the granular metal−insulator films composed of magnetic metal particles embedded in nonmagnetic matrix, the MCD can be well fitted with an equation developed from the effective medium approximation and Maxwell−Garnett theory.[25] This theory was fitted to the Co/ZnO (3.0 nm) and Co/ZAO (3.0 nm) films as shown in Figure 4. It is found that there exists an obvious deviation between the fit and the experimental data in the high energy region. This implies that metallic Co particles are not solely responsible for the observed MCD spectra and there is a contribution originating from the magnetism of the semiconductor matrix which is overwhelming the positive signal expected from metallic Co particles in the MCD spectra. In addition, the characteristic d−d transition at 2 eV observed in T_d symmetry assigned to excitation from $^4A_2$ (F) to ^2E (G) and $^4T_1$ (P) for Co^{2+} ions is blurred out in these amorphous films.[26] Therefore, we speculate that the magnetic semiconductors are formed at the interface between Co metal and semiconductor matrix probably because the Co^{2+} ions substitute for Zn^{2+} ions in the ZnO lattice by interdiffusion. The magnetism of the films comes from the dispersed superparamagnetic Co particles and the interfacial magnetic semiconductors. This result is in good agreement with the blurred interface between Co nanoparticles and semiconductor matrix in Figure 1. Compared to the Co/ZnO (3.0 nm) film, the larger deviation of the Co/ZAO (3.0 nm) film in the high energy region indicates that the contribution of the magnetic semiconductors to the magnetism of the Co/ZAO film is stronger than that of the Co/ZnO film, which is consistent with the larger magnetization of the Co/ZAO films and the positive Curie−Weiss temperature. The enhanced magnetization for the Al doped films is probably due to the enhanced magnetism of the interfacial magnetic semiconductors with increasing carrier concentration.[13,27] In our samples, the resistivity of the Co/ZnO films with $x = 1.0$ and 3.0 are 0.85 and 33.60 Ω·cm, respectively, whereas those of the Co/ZAO films are considerably lower, 0.08 and 0.26 Ω·cm, respectively.

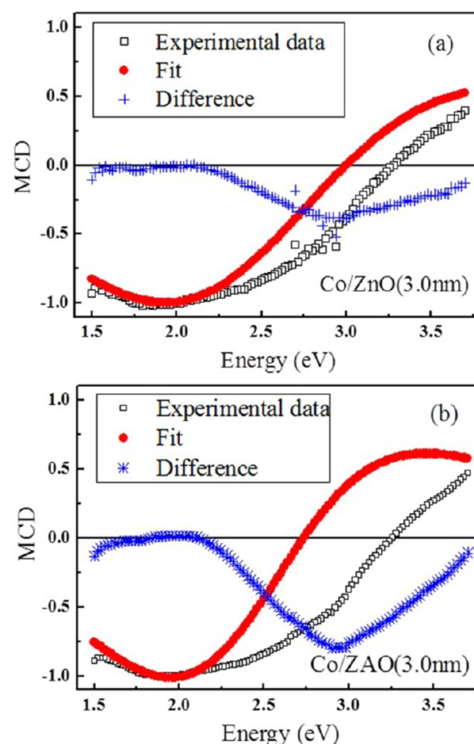

Figure 4. Normalized MCD spectra taken in $H = 18$ kOe at RT for the Co/ZnO (3.0 nm) film (a) and Co/ZAO (3.0 nm) film (b). The fits of MCD data were calculated using the effective medium approximation and Maxwell−Garnett theory written as $\varepsilon_{xy}^{eff} = f((\varepsilon_{xy}^{Co})/((1 + (1 - f)((\varepsilon_{xx}^{Co} - \varepsilon_{xx}^{ZnO(ZAO)})/(\varepsilon_{xx}^{ZnO(ZAO)}))L_x)^2))$, where ε_{xy}^{eff} is the off diagonal component of the effective dielectric tensor, f is the volume fraction of metallic Co, and L_x is a shape factor. $\varepsilon_{xx}^{ZnO(ZAO)}(\omega)$ was calculated using the method described by Sun et al.[28] with plasma frequency $\omega_p = 9.74$ eV and cyclotron frequency $\omega_c = 0.089$ eV.[29] For the Co/ZnO (3.0 nm) film, $L_x = 0.33$, $f_{Co/ZnO} = 0.008$, and relaxation time $\tau = 0.21$; for the Co/ZAO (3.0 nm) film, $L_x = 0.28$, $f_{Co/ZAO} = 0.027$, and $\tau = 0.305$.

From the result of fit in Figure 4, it can be seen that the volume fraction of metallic Co (f) is very small ($f_{Co/ZnO} = 0.008$; $f_{Co/ZAO} = 0.027$) in those two films. These very small volume fractions of metallic Co are actually consistent with well separated metallic regions as can be seen in the TEM for the films with smaller semiconductor fraction, Co/ZnO (1.0 nm) and Co/ZAO (1.0 nm). The maximum volume fraction of metallic Co can be calculated according to the nominal structure of the films (i.e, Co (0.6 nm)/ZnO (3.0 nm) and Co (0.6 nm)/ZAO (3.0 nm)). The value of ∼0.17 is obtained, which is larger than the value of f obtained from fitting the MCD data. This means that most of the Co is dispersed in semiconductors in the Co/ZnO and Co/ZAO films with $x = 3.0$.

XPS is well-known to be sensitive to the chemical environment, which might provide information for the chemical state of the cobalt. To understand the correlation of structure and magnetism in detail, the Co 2p core-level XPS spectrum of the Co/ZAO film with $x = 3.0$ was taken after the surface was cleaned by Ar^+ sputtering (see Figure 5). The charge-shifted spectrum was corrected using the maximum of the adventitious C 1s signal at 284.8 eV. The spectrum exhibits six Co 2p peaks including two $2p_{3/2}$ peaks, two $2p_{1/2}$ peaks, and their two satellite peaks as shown in Figure 5. The Co 2p spectrum exhibits primary Co $2p_{3/2}$ and Co $2p_{1/2}$ peaks at 780.4 and

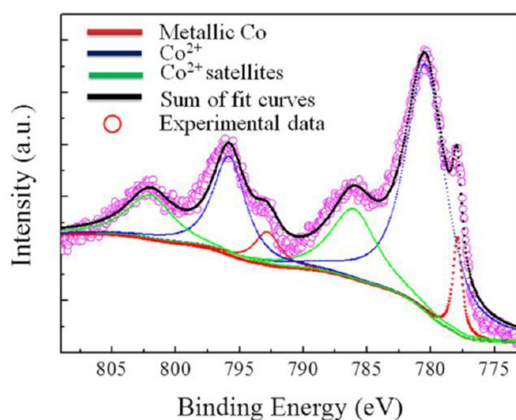

Figure 5. Co 2p core-level XPS spectrum of the Co/ZAO (3.0 nm) film after removing the topmost ∼3 nm by Ar^+ sputtering. The obtained XPS spectra are fitted using the Gaussian method.

795.6 eV, respectively, accompanied by respective satellite peaks at higher binding energy, which match with Co^{2+} ions. The minor peaks with the binding energy at 778.0 and 792.8 eV with energy difference of 14.8 eV between them originate from Co metal.[30,31] This indicates that most Co exists as Co^{2+} ions and there are only a small number of metallic Co particles, which is in agreement with the fitting value of f in MCD data. Also, the metallic Co atomic concentration can be calculated from the XPS spectrum. The $2p_{3/2}$ peak integral area ratio of Co^{2+} ions to metallic Co is ∼6.89 for the Co/ZAO (3.0 nm) film as shown in Figure 5, and the Zn/Co atom ratio of ∼2.1 can be obtained from XPS data. Therefore, the metallic Co atomic concentration of the Co/ZAO (3.0 nm) film is equal to $1/(1 + 2.1) \times 1/(1 + 6.89) = 4.09\%$. This value can be converted to the volume concentration of ∼2.4%, which is similar to that from MCD fitting.

According to the data of TEM, ZFC−FC, MCD, and XPS, we consider that the films consist of superparamagnetic Co nanoparticles, semiconductor matrix, and the interfacial magnetic semiconductors consisting of $Zn_{1-x}Co_xO$ (x varies between the solubility limit for Co in ZnO and zero). Figure 6 shows a schematic view of this picture. Also, a comparison for Figures 2 and 3a,b shows that the MR has a much slower dependence on magnetic field than the magnetization measured at the same temperature (at RT) for the four films.[32,33] This phenomenon may be ascribing to the existence of the paramagnetic free Co^{2+} ions in the semiconductor matrix (see Figure 6), producing nonsaturated MR curve. This is known from the X-ray magnetic circular dichroism spectroscopy in Co−Li codoped and Co doped ZnO films in which only paramagnetic Co^{2+} has been found.[34,35] The total moment signal of the Co/ZnO (1.0 nm) film and the substrate signal after removing the film were also measured with 1.8 T maximum field. We obtained the net moment of the Co/ZnO (1.0 nm) film with a residual moment increasing with field (as shown in Figure 7a), which may be responsible for the tail in the MR curve. The MR value for the granular films is directly proportional to the square of the normalized magnetization, $(M/Ms)^2$ (ref 36). For the Co/ZnO (1.0 nm) film, the calculated $(M/Ms)^2$ using the net moment in Figure 7a is expressed as the hollow block in Figure 7b and is quite consistent with the MR experimental value. In the case of nonsaturated MR curves, the same results were reported in other granular compounds and it is attributed to spin tunneling in magnetically disordered regions between grains[37] or the disordered magnetic surface of grain.[38]

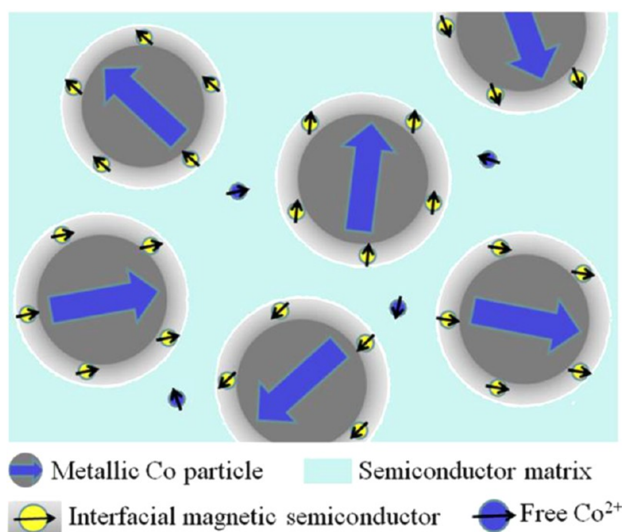

Figure 6. Schematic illustration of the granular films consisting of Co particles, semiconductor matrix, and the interfacial magnetic semiconductors.

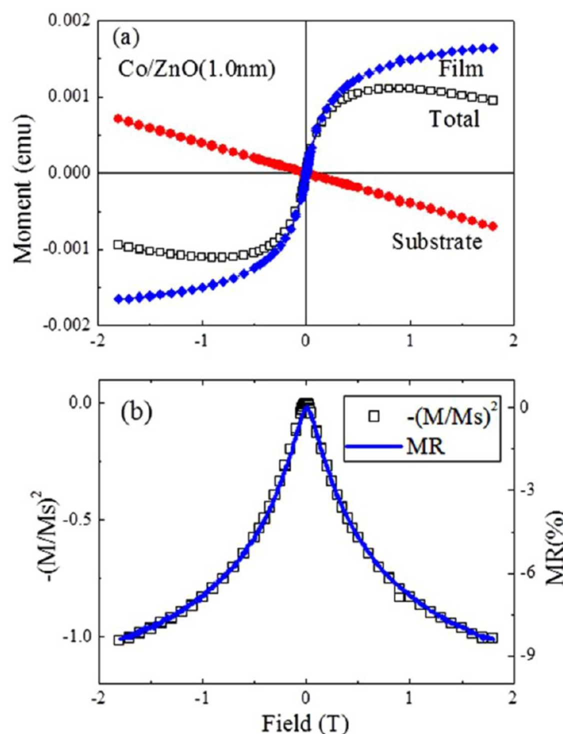

Figure 7. (a) Magnetic field dependence of the net moment, the substrate signal, and the total signal of the Co/ZnO (1.0 nm) film. (b) Relation between MR and $-(M/Ms)^2$ for the Co/ZnO (1.0 nm) film.

As mentioned above, although our analysis of the interfacial magnetic semiconductors gives only a qualitative picture, the large tunneling MR effect and high spin polarization in our films are most likely related to the interfacial magnetic semiconductors, which help the tunneling electrons to overcome the conductivity mismatch between Co metal and semiconductor matrix. The reason may be the fact that the

dx.doi.org/10.1021/am303276b | ACS Appl. Mater. Interfaces 2013, 5, 3607−3613

interfacial magnetic semiconductors can provide different tunnel barrier heights for spin-up and spin-down electrons due to the spin splitting of impurity band,[11] acting as the spin filter.[39] In order to further explore the spin filter effect of the magnetic semiconductors between metallic Co and ZnO semiconductor, the Co (50 nm)/ZnO (20 nm) heterostructure was fabricated by sputtering under the same condition of the Co/ZnO films; then, ~10 nm thick Ag electrode was deposited on ZnO layer by sputtering. The schematic diagram of the Co (50 nm)/ZnO (20 nm)/Ag (10 nm) junction with an interfacial magnetic semiconductor between metallic Co and ZnO layer is shown in the inset of Figure 8. A small negative

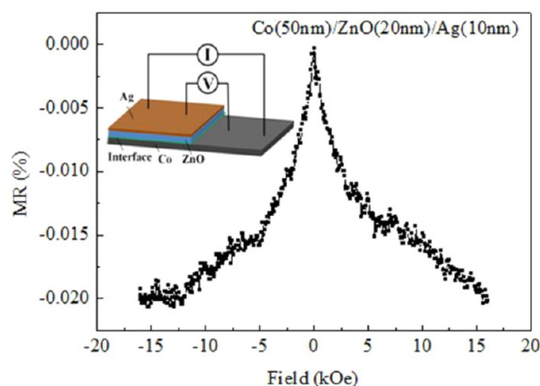

Figure 8. MR as a function of field for the glass/Co (50 nm)/ZnO (20 nm)/Ag (10 nm) junction measured at RT. The inset shows the same heterostructure schematic diagram.

MR effect in this junction with one magnetic electrode is observed and measured in field in the plane at RT, indicating that the tunnel current through the interfacial magnetic semiconductors is spin polarized and the interfacial magnetic semiconductors act as a spin filter barrier.[40] The reason of the small value of MR, which may be related to the pinholes or defects or roughness in the interface (large junction areas of 0.5 × 0.5 cm^2), is not yet understood completely, and future experiments are planned to study the spin filter effect of the interfacial magnetic semiconductors.

4. CONCLUSIONS

In conclusion, the structure, magnetism, and MR of the Co/ZnO and Co/ZAO films made by sputtering were investigated. The films comprise metallic Co nanoparticles, semiconductor matrix, and an interfacial magnetic semiconductor between Co particles and the semiconductor matrix proved by TEM, ZFC−FC, MCD, and XPS. The magnetism of the films originates from both the metallic Co particles and the interfacial magnetic semiconductors. The maximum RT MR value of a Co/ZAO granular film with x = 1.0 reaches −12.3%, and the corresponding spin polarization of tunneling electrons is about 37.5% estimated by Inoue−Maekawa model, comparable to bulk cobalt. The robust spin injection from metallic Co particles into the semiconductor matrix may be due to the formation of the magnetic semiconductor ZAO with enhanced conductivity and magnetism at the interface between Co particles and semiconductor matrix. A small RT MR ratio has been obtained for a Co/ZnO/Ag structure, suggesting the spin filtering of the interfacial magnetic semiconductors. These results indicate that inserting a magnetic semiconductor is a very promising method to improve the spin injection efficiency into the semiconductors.

AUTHOR INFORMATION

Corresponding Author

*E-mail: xuxh@dns.sxnu.edu.cn.

Notes

The authors declare no competing financial interest.

ACKNOWLEDGMENTS

The work is financially supported by NSFC (51025101 and 11274214), the Special Funds of Shanxi Scholars Program, the Ministry of Education of China (IRT 1156 and RFDPHE 20121404130001), and the Youth Science Foundation of Shanxi Province (2012021020-2).

REFERENCES

(1) Schmidt, G.; Ferrand, D.; Molenkamp, L. W.; Filip, A. T.; van Wees, B. J. *Phys. Rev. B* **2000**, *62*, R4790−R4793.
(2) Rashba, E. I. *Phys. Rev. B* **2000**, *62*, R16267−R16270.
(3) Jiang, X.; Wang, R.; Shelby, R. M.; Macfarlane, R. M.; Bank, S. R.; Harris, J. S.; Parkin, S. S. P. *Phys. Rev. Lett.* **2005**, *94*, 056601.
(4) Fert, A.; Jaffrès, H. *Phys. Rev. B* **2001**, *64*, 184420.
(5) Moodera, J. S.; Hao, X.; Gibson, G. A.; Meservey, R. *Phys. Rev. Lett.* **1988**, *61*, 637−640.
(6) Filip, A. T.; LeClair, P.; Smits, C. J. P.; Kohlhepp, J. T.; Swagten, H. J. M.; Koopmans, B.; de Jonge, W. J. M. *Appl. Phys. Lett.* **2002**, *81*, 1815−1817.
(7) Smits, C. J. P.; Filip, A. T.; Kohlhepp, J. T.; Swagten, H. J. M.; Koopmans, B.; de Jonge, W. J. M. *J. Appl. Phys.* **2004**, *95*, 7405−7407.
(8) Müller, M.; Luysberg, M.; Schneider, C. M. *Appl. Phys. Lett.* **2011**, *98*, 142503.
(9) Gould, C.; Schmidt, G.; Richter, G.; Fiederling, R.; Grabs, P.; Molenkamp, L. W. *Appl. Surf. Sci.* **2002**, *190*, 395−402.
(10) Pan, F.; Song, C.; Liu, X. J.; Yang, Y. C.; Zeng, F. *Mater. Sci. Eng. R* **2008**, *62*, 1−35.
(11) Coey, J. M. D.; Venkatesan, M.; Fitzgerald, C. B. *Nat. Mater.* **2005**, *4*, 173−179.
(12) Hao, W.; Li, J.; Xu, H.; Wang, J.; Wang, T. *ACS Appl. Mater. Interfaces* **2010**, *2*, 2053−2059.
(13) Xu, X. H.; Blythe, H. J.; Ziese, M.; Behan, A. J.; Neal, J. R.; Mokhtari, A.; Ibrahim, R. M.; Fox, A. M.; Gehring, G. A. *New J. Phys.* **2006**, *8*, 135.
(14) Liu, X. C.; Shi, E. W.; Chen, Z. Z.; Zhang, H. W.; Xiao, B.; Song, L. X. *Appl. Phys. Lett.* **2006**, *88*, 252503.
(15) Liu, X. J.; Song, C.; Zeng, F.; Pan, F. *J. Phys.: Condens. Matter.* **2007**, *19*, 296208.
(16) Qi, S.; Jiang, F.; Fan, J.; Wu, H.; Zhang, S. B.; Gehring, G. A.; Zhang, Z.; Xu, X. *Phys. Rev. B* **2011**, *84*, 205204.
(17) Yan, S. S.; Ren, C.; Wang, X.; Xin, Y.; Zhou, Z. X.; Mei, L. M.; Ren, M. J.; Chen, Y. X.; Liu, Y. H.; Garmestani, H. *Appl. Phys. Lett.* **2004**, *84*, 2376−2378.
(18) Chen, G.; Zeng, F.; Pan, F. *Appl. Phys. Lett.* **2009**, *95*, 232508.
(19) Quan, Z.; Liu, W.; Li, X.; Xu, X.; Addison, K.; Score, D. S.; Gehring, G. A. *Mater. Lett.* **2011**, *65*, 2982−2984.
(20) Quan, Z. Y.; Xu, X. H.; Li, X. L.; Feng, Q.; Gehring, G. A. *J. Appl. Phys.* **2010**, *108*, 103912.
(21) Sheng, P.; Abeles, B.; Arie, Y. *Phys. Rev. Lett.* **1973**, *31*, 44−47.
(22) Inoue, J.; Maekawa, S. *Phys. Rev. B* **1996**, *53*, R11927−R11929.
(23) Upadhyay, S. K.; Palanisami, A.; Louie, R. N.; Buhrman, R. A. *Phys. Rev. Lett.* **1998**, *81*, 3247−3250.
(24) Huang, J. C. A.; Hsu, H. S.; Hu, Y. M.; Lee, C. H.; Huang, Y. H.; Lin, M. Z. *Appl. Phys. Lett.* **2004**, *85*, 3815−3817.
(25) Clavero, C.; Cebollada, A.; Armelles, G.; Huttel, Y.; Arbiol, J.; Peiró, F.; Cornet, A. *Phys. Rev. B* **2005**, *72*, 024441.
(26) Fukuma, Y.; Asada, H.; Yamamoto, J.; Odawara, F.; Koyanagi, T. *Appl. Phys. Lett.* **2008**, *93*, 142510.

(27) Behan, A. J.; Mokhtari, A.; Blythe, H. J.; Score, D.; Xu, X. H.; Neal, J. R.; Fox, A. M.; Gehring, G. A. *Phys. Rev. Lett.* **2008**, *100*, 047206.
(28) Sun, X. W.; Kwok, H. S. *J. App. Phys.* **1999**, *86*, 408−411.
(29) Krinchik, G. S. *J. App. Phys.* **1964**, *35*, 1089−1092.
(30) Moulder, J. F.; Strickle, W. F.; Sobol, P. E.; Bomben, K. D. In *Handbook of X-ray Photoelectron Spectroscopy*, 2nd ed.; Chastain, J., Ed.; Perkin-Elmer: Eden Prairie, MN, 1992; p 82−83.
(31) Ney, A.; Opel, M.; Kaspar, T. C.; Ney, V.; Ye, S.; Ollefs, K.; Kammermeier, T.; Bauer, S.; Nielsen, K.-W.; Goennenwein, S. T. B.; Engelhard, M. H.; Zhou, S.; Potzger, K.; Simon, J.; Mader, W.; Heald, S. M.; Cezar, J. C.; Wilhelm, F.; Rogalev, A.; Gross, R.; Chambers, S. A. *New J. Phys.* **2010**, *12*, 013020.
(32) Chien, C. L.; Xiao, J. Q.; Jiang, J. S. *J. Appl. Phys.* **1993**, *73*, 5309−5314.
(33) Mitani, S.; Fujimori, H.; Ohnuma, S. *J. Magn. Magn. Mater.* **1997**, *165*, 141−148.
(34) Tietze, T.; Gacic, M.; Schütz, G.; Jakob, G.; Brück, S.; Goering, E. *New J. Phys.* **2008**, *10*, 055009.
(35) Ney, A.; Ollefs, K.; Ye, S.; Kammermeier, T.; Ney, V.; Kaspar, T. C.; Chambers, S. A.; Wilhelm, F.; Rogalev, A. *Phys. Rev. Lett.* **2008**, *100*, 157201.
(36) Xiao, J. Q.; Jiang, J. S.; Chien, C. L. *Phys. Rev. Lett.* **1992**, *68*, 3749−3752.
(37) Serrate, D.; De Teresa, J. M.; Algarabel, P. A.; Ibarra, M. R.; Galibert, J. *Phys. Rev. B* **2005**, *71*, 104409.
(38) Serrate, D.; De Teresa, J. M.; Algarabel, P. A.; Fernández-Pacheco, R.; Galibert, J.; Ibarra, M. R. *J. Appl. Phys.* **2005**, *97*, 084317.
(39) Lüders, U.; Bibes, M.; Bouzehouane, K.; Jacquet, E.; Contour, J.-P.; Fusil, S.; Bobo, J.-F.; Fontcuberta, J.; Barthélémy, A.; Fert, A. *Appl. Phys. Lett.* **2006**, *88*, 082505.
(40) LeClair, P.; Ha, J. K.; Swagten, H. J. M.; Kohlhepp, J. T.; van de Vin, C. H.; de Jonge, W. J. M. *Appl. Phys. Lett.* **2002**, *80*, 625−627.